Quasi-two-dimensional fluctuations in the magnetization of La_{1.9}Ca_{1.1}Cu_{2}O_{6+δ} superconductors

Xiaoya Shi, I. K. Dimitrov, Toshinori Ozaki, Genda Gu, and Qiang Li

Phys. Rev. B **96**, 184519 — Published 21 November 2017

DOI: 10.1103/PhysRevB.96.184519

Quasi-two-dimensional fluctuations in the magnetization of $La_{1.9}Ca_{1.1}Cu_2O_{6+\delta}$ superconductors

Xiaoya Shi[1,*], I. K. Dimitrov[1,2,*,†], Toshinori Ozaki[1,3], Genda Gu[1], and Qiang Li[1,†]

[1]Condensed Matter Physics and Materials Science Division, Brookhaven National Laboratory, Upton, NY 11973-5000, USA
[2]System Evaluation Division, Institute for DefenseAnalyses, Alexandria, VA 22311, USA
[3] Department of Nanotechnology for Sustainable Energy, Kwansei Gakuin University, 2-1 Gakuen, Sanda, Hyogo 660-1337, Japan

Abstract

We report the results of magnetization measurements with the magnetic field applied along the *c*-axis on superconducting $La_{1.9}Ca_{1.1}Cu_2O_{6+\delta}$ single crystals processed under ultra high oxygen pressure. Strong fluctuation effects were found in both low and high field regimes. Scaling analysis of the high field magnetization data near the critical temperature (T_c = 53.5 K) region reveals the characteristics of critical fluctuation behavior of quasi-two-dimensional (2D) superconductivity, described by Ginzburg-Landau theory using the Lowest Landau Level approximation. Low field magnetic susceptibility data can be successfully explained by the Lawrence-Doniach model for a quasi-2D superconductor, from which we obtained the *ab* plane Ginzburg-Landau coherence length of this system, $\xi_{ab}(0)$ = 11.8 ± 0.9 Å. The coherence length along the *c*-axis, $\xi_c(0)$, is estimated to be about 1.65Å, which is in-between those of 2D cuprate systems, such as $Bi_2Sr_2Ca_2Cu_3O_{10}$ and $Bi_2Sr_2CaCu_2O_8$, and quasi-3D cuprate systems, such as overdoped $La_{2-x}Sr_xCuO_4$ and $YBa_2Cu_3O_{7-\delta}$. Our studies suggest a strong interplay among the fluctuation effects, dimensionalities, and the ratios of the interlayer Cu-O plane spacing, *s*, to the *c*-axis coherence lengths. A high $s/\xi_c(0)$ was observed in the high pressure oxygenated $La_{1.9}Ca_{1.1}Cu_2O_{6+\delta}$, and that apparently drives this system to behave more like a quasi-2D superconductor.

[*] These authors contributed equally to this work
[†] Corresponding authors: qiangli@bnl.gov (QL), idimitro@ida.org (IKD)

I. Introduction:

The discovery of high-T_c superconductivity in the La-Ba-Cu-O system by Bednorz and Müller[1] started an avalanche of scientific discovery which has persisted to the present days. High-T_c superconductors (HTS) are essential not only for applications, but also for serving as a testbed of fundamental physics problems, such as studies of exotic quantum effects[2] and order-disorder transitions[3,4]. Two of the best-known families of high-T_c materials: bismuth strontium calcium copper oxide (BSCCO) based, such as $Bi_2Sr_2Ca_2Cu_3O_{10}$ (Bi2223) and $Bi_2Sr_2CaCu_2O_{8,}$ (Bi2212) and rare-earth barium copper oxide (REBCO) based, such as $YBa_2Cu_3O_{7-\delta}$, are characterized by layered (perovskite) structures, where the superconductivity takes place in the copper oxide planes.[5] However, a major distinction between these two families is that the *c* lattice constant in YBCO (orthorhombic unit cell) is ~ 11.6 Å, while in BSCCO the *c* lattice constant is on the order of 30.9 Å (in Bi2212).[6] In BSCCO, this characteristic distance far exceeds the superconducting coherence length, ξ, and is one of the factors essential for the rise to 2D superconductivity.

The transverse spatial correlations in BSCCO at high magnetic fields are limited by the field and the quasi-particles to low Landau levels.[7] This confinement reduces the dimensionality of the system and increases the importance of the phase fluctuations in the order parameter.[7,8] It has been shown that the fluctuations at the lowest Landau levels (LLL) effectively dominate the *H*–*T* superconducting phase diagram above a characteristic field $\overline{H}(T) = (1/3)H_{c2}(T) + (\sqrt{G_i}/3)[\overline{H}(T)H_{c2}(0)T/T_{c0}]^{1/2}$ in a 2D system,[7] where $H_{c2}(T)$, T and T_{c0} stand for the upper critical field, temperature and the mean-field transition temperature at zero field, respectively. The scaling properties of the Ginzburg Landau Lowest Landau Levels (GL-LLL) theory suggest that the free energy obeys the form: $F(T,H) = THf(At)$, where $f(At)$ is a scaling function of the field and a temperature-dependent variable $t = [T - T_c(H)]/(TH)^n$ (n = 1/2 or 2/3 for a 2D or 3D system, respectively). The 3D scaling behavior was shown in YBCO single crystals in magnetization,[8] electrical conductivity,[9] Ettinghauser effect,[10] and specific heat[11] measurements.

Magnetization studies have also been pivotal in revealing the quasi-two-dimensional character of the high-T_c superconductivity in the BSCCO family, both in the decade following its discovery,[12–21] as well as in more recent times.[22] One of the better-known signatures associated with fluctuation-induced magnetization is the so-called "crossing point" effect, *i.e.*, all the temperature-dependent magnetization scans for different fields (applied parallel to the crystallographic *c*-axis) cross each other at a given point at a temperature near the critical temperature, T_c.[23] This crossing point has been ubiquitously observed in BSCCO, and more specifically – in Bi2212[12–14]and Bi2223[15–17]as well as in some Tl-based cuprates[18,22]. A number of theories have emerged attempting to explain the crossing point effect: Bulaevskii, Ledvij and Kogan dealt with the low magnetic field ($H \leq 1$ T) limit and suggested it to be a result of the positional fluctuation of vortices,[19] while Tešanović *et al*. suggested that the crossing at high fields ($H \gg 1$ T) is due to phase fluctuations of the superconducting order

parameters.[20] Particularly good has been the agreement between these theories and experimental data taken with *H* parallel to the *c* axis.[14–18]

The lanthanum calcium copper oxide [among which, $La_2CaCu_2O_6$ (La2126)] family has been shown to be the simplest bilayer structure among the copper oxide superconductors (see Fig. 1).[24] In a stoichiometric compound (La2126, as shown in Fig. 1a), the interstitial oxygen site O (3) marked in Fig. 1b is not occupied. High pressure oxygen annealing has been shown to introduce interstitial oxygen on to the O (3) site, which effectively bridges two CuO_5 pyramids in a bilayer to two CuO_6 octahedra as shown in Fig. 1b. La2126 has neither the additional carrier reservoir layers in the superconducting compounds of Bi2212 and $Tl_2Sr_2CaCu_2O_8$ (Tl2212), nor the square planar Cu-O chain in the superconducting compound of YBCO.[24] Furthermore, high oxygen pressure annealed $La_2CaCu_2O_{6+\delta}$(La2126+δ) is still a bilayer system, and a bilayer cuprate is thought to be a typical example of a stronger coupling within the bilayer and a relatively weak one between bilayers.[25] The dimension of the conducting bilayer in La2126+δ has been known to lie between those of the conduction layers in YBCO and BSCCO, raising the question as to whether the La2126+δ system will display superconductivity closer to YBCO (3D) or BSCCO (2D).

Here, we report the analysis results of a magnetization measurement on a $La_{1.9}Ca_{1.1}Cu_2O_{6+\delta}$ single crystal, and thereby we show that the scaled form of the magnetization at high-fields suggests the presence of a two-dimensional superconductivity according to the GL-LLL fluctuation theory. Furthermore, based on the Lawrence-Doniach model, the low-field magnetic susceptibility was shown to behave more like a quasi-2D system. Comparing the superconducting parameters obtained from the scaling results in this work with those reported for the traditional 2D BSCCO and 3D YBCO, it is interesting to note that (*i*) the large anisotropy, and (*ii*) the large ratio of effective spacing of the superconducting layers to the $\xi_c(0)$, are essential for 2D superconductivity while the opposite is true for 3D superconducting behavior. Although the high oxygen pressure annealed $La_{1.9}Ca_{1.1}Cu_2O_{6+\delta}$ crystal exhibits similar anisotropy to that of YBCO, it still behaves more like a 2D superconductor, suggesting the importance of the ratio of effective spacing of superconducting layers to the $\xi_c(0)$, which is properly related to the crystal structure.

The paper is organized as follows: In Section II we present the preparation of the experimental sample along with the synthesis conditions for its making and the conditions for the magnetization measurements performed. In Section III we present the data analysis on the magnetization data, with a discussion of the scaling behavior of our La2126 sample, and its implications on the superconductivity. Finally, we finish with a brief summary section which recaps our findings and conclusions.

II. Materials and Methods:

A. Materials Synthesis

A single crystal $La_{1.9}Ca_{1.1}Cu_2O_{6+\delta}$ was grown by the floating zone method. The crystal was grown under oxygen pressures of 11 bars. The details of the crystal growth have been

reported elsewhere.[24] The as-grown single crystal was annealed under 1400 bars oxygen pressure at 1200 ºC for 10 hours. The X-ray diffraction pattern of the sample reveals the crystallographic dimensions of the unit cell, which are as follows: $a = b = 3.8578(8)$ Å and $c = 19.967(4)$ Å. We have used transmission electron microscopy (TEM) techniques to compare the structure of superconducting crystals with the as-grown, non-superconducting starting material. A minority non-superconducting phase (less than 2%) of $La_{2-x}Ca_xCuO_4$ (La-214) is detected. Layers of the La-214 phase are found to be coherently interspersed along the *c*-axis direction of the primary La-2126 phase. The occurrence of the La-214 intergrowth-like defects does not seem to harm the superconductivity of the La-2126 phase, nor does it change the overall magnetization behavior and our interpretations.

B. Magnetization Measurements

The large crystal used in our study weighed 271 mg. All magnetization, *M*, measurements were carried out in a field applied parallel to the crystalline *c*-axis by using a superconducting quantum interference device (SQUID) magnetometer by Quantum Design, *Inc*. with a 6-cm scan length, where the field inhomogeneity was estimated to be no more than 0.005 %. The reversible magnetization data were taken by measuring the magnetic moment versus temperature from the irreversible temperature data up to 300 K. A 2-min delay was introduced after each temperature change to stabilize the system, so that the system temperature was always within ±0.02 K of the target temperature prior to measurement. An accuracy of better than 2×10^{-6} emu (equivalent to 6×10^{-4}Oe for the value of $4\pi M$) for magnetic momenta was obtained. The linear magnetization data were fitted from 90 K to 130 K as the baseline, which was utilized to correct for the background and normal-state contributions of the magnetization results.[7,15] It was also noticed that there is a phase transition point around 150 K, which greatly influences the magnetization. And our fitting points are far away from the transition area. We note that the results in this study are not artifacts of a specific form of the normal-state background.

III. Results and Discussion:

We performed magnetization measurements with zero-field cooled (ZFC) and field-cooled (FC) thermal histories on the La2126+δ single crystal at a field of 2 Oe with the magnetic field applied parallel to the *c*-axis (see Fig. 2a). Due to the large and irregular size of the sample, it is necessary to rescale the real field *H* by taking into account the demagnetization factor *N* according to $H = H_a - NM$, where H_a is the external field which is 2 Oe here. The resulting $M(H)$ curve for $H \parallel c$ is shown in Fig. 2b, from which we estimate *N* to be 0.542 for $H \parallel c$ and apply the value for plotting Fig. 2a. The slope of the fitted line in the linear region is -0.985(5) $\approx$ -1, which is very close to the Meissner line plotted in Fig 2b, suggesting the full shielding within the Cu-O plane. The critical temperature, $T_c = 53.5$ K, was obtained by linearly extrapolating the $4\pi M/H(T)$ data to the zero line, while another linear fit through the bottom horizontal line was used to define the transition width ($\Delta T_c \sim 1.5$ K). We note that a small step-like feature was observed around 12.5 K (see Inset of Fig.2a),

indicating flux penetration into small defects in these crystals. Our sample comprises large single-crystal domains with the unavoidable presence of a very small amount of a CaO secondary phase, which is embedded in the La2126 matrix.[24] Actually, according to the result shown in Fig. 2a, the superconducting volume of our crystal is around 89.2 % and is estimated to contain roughly 2% of superconducting secondary phases (T_c ~ 12.5 K) by volume which agrees with previous observations.[28,29] Such a small amount of defects is not expected to have a significant influence on the magnetization behavior of the crystal around or above the T_c region.

The magnetization, M, was measured at fields of 10,000 Oe, 30,000 Oe and 50,000 Oe, applied parallel to the c-axis (see Fig. 3 for a plot of $4\pi M$ versus temperature). The well-defined crossover behavior of various $4\pi M(H, T)$ versus T curves is clearly shown in the figure as evidence of the strong fluctuation effects present. The crossing point was found at the same location for each $4\pi M(H, T)$ versus T curve within experimental error, where the crossing-point temperature, T^*, was shown to be $T^* = 51.0 \pm 0.2$ K, and crossing-point magnetization, $4\pi M^* = -1.3 \pm 0.1$ G. At fields near the $H_{c2}(T)$ line, this crossover behavior was defined to be the result of the entropy associated with the fluctuation of vortices by Tešanović *et al*.[20] The vortex positions (or the phase fluctuation of the superconducting order parameter) at low fields (near $T_c(H)$) are important, while the amplitude fluctuations become significant in the high-field regime (near the $H_{c2}(T)$ line).[14]

Similar critical fluctuations in the thermodynamics of *quasi*-2D type-II superconductors have been extensively studied and described in terms of a non-perturbative scaling theory, as long as the description of Ginzburg-Landau (GL) field theory on a degenerate manifold spanned by the lowest Landau levels (LLL) for Copper pairs is valid (GL-LLL).[20] The GL-LLL scaling in the case of a 2D system has suggested that in the vicinity of the upper critical field, $H_{c2}(T)$, the free energy, $F(T, H)$, scales with the field and temperature as $F(T,H) = THf(At)$, where $f(At)$ is a scaling function of the temperature-dependent variable $t = [T - T_c(H)]/(TH)^{1/2}$ and A is a numerical constant.[20,30,31] This theory, has been widely and successfully used for scaling the Bi-based high-temperature superconductors with 2D critical fluctuation behavior, which has furthermore provides an explicit closed-form expressions for the scaling functions of the free energy, $f(x)$, as well as for the magnetization, entropy, and specific heat.[14,20] In the particular case of the magnetization, the scaling functions are given by:[20]

$$\frac{F(T,H)}{TH} s\phi_0 = f(x), \quad x = At, \quad A = a'(\phi_0 s / 2b)^{1/2} U_0,$$

$$f(x) = -\frac{1}{2}x^2 + \frac{1}{2}x\sqrt{x^2+2} + \sinh^{-1}(x/\sqrt{2}), \tag{1}$$

$$\frac{M(H,T)}{\sqrt{HT}} \frac{s\phi_0 H'_{c2}}{A} = -f'(x) = x - \sqrt{x^2+2}, \tag{2}$$

where a and b are the GL coefficients, ϕ_0 is flux quantum (equals to $hc/2e$), s is effective

spacing of the superconducting layers and U_0 (U_0 = 0.8 around $H_{c2}(T)$ [14]) is the vortex interaction constant.[20] As shown in Eq. (2), the only adjustable parameters involved are H'_{c2} and T_{c0}, where $H'_{c2} = \left| dH_{c2} / dT \right|$ at $T = T_{c0}$.

In order to ascertain the dimensionality of the superconductivity, we scaled the magnetization versus temperature data according to 2D and 3D theories (see Fig. 4).[20] Fig.4a shows a plot of the scaled fluctuation magnetization under 2D behavior, where only the high field data at 10,000, 30,000, and 50,000 Oe are plotted for clarity. The fitting temperature region used in this study is in the temperature regime $T \geq T_{c0} - 3H / H'_{c2}$, where the scaling theory applies. The optimum fit yields T_{c0} = 54.2 K and $H'_{c2} = 3.33$ T/K. It was also noticed that the scaling behavior of the data was much more sensitive to the T_{c0} value than the choice of H'_{c2}, which was also observed in the scaling of other *quasi*-2D systems reported.[14] Thus, the H'_{c2} value could range from 3.18 to 3.65 without any distinguished changes between the curves, while only 1% of the change in T_{c0} could significantly distort the scaling plot. Fig. 4a shows how all lines neatly fall onto one single curve using 2D scaling, which strongly suggests that our sample is very close to *quasi*-2D behavior. As for a comparison, an assumed 3D scaling fitting, for which universal curves of the form $M/(TH)^{2/3}$ versus $[T - T_c(H)] / (TH)^{2/3}$ are expected, is also performed and shown in Fig. 4b. Fig. 4b clearly shows that the splitting near the transition region for different fields inevitably exists, with any choice of H'_{c2} and T_{c0}. Thus, 3D scaling does not work as well as the 2D scaling near the transition region, which demonstrates that the superconducting transition of La2126+δ is 2D in nature.

Furthermore, based on the static models proposed by Lawrence and Doniach, Klemm, and Prober and Beasley,[15] the temperature dependence of the weak-field fluctuation diamagnetic susceptibility, $\chi(T)$, above T_c will exhibit the relationship $\chi(T) / T \propto T_c / (T - T_c)^n$, where n is 1 for a 2D system, and 1/2 for a 3D system. This relation is only valid in the weak-field regime defined by Klemm,[32] which corresponds to $B < S_0 = \phi_0 / (sL)$, where L is the effective length in the *ab* plane, which is of the same order of magnitude as the average grain size (~ 10 μm) and we take half of the unit cell parameter for the *s* value here. As a result, the weak-field regime here is around several kOe for the applied field. We studied the temperature dependence of T/χ at 300 Oe and 500 Oe, which is shown in Fig. 5a. The data show very close linear behavior at both fields between 58 K and 63 K. In principle, a linear behavior is expected for the 2D system based on the model. Our data indicate that the La2126+δ system behaves more like a 2D system. The mean-field transition temperature, $T_c^{MF} = 58.13(5)$ K, was obtained as the intercept of the straight line in Fig.5a, which is 4.6 K higher than that from a 2-Oe shielding measurement. Fig. 5b shows a fit of a 2D LD model to the data for $\chi(T)$ with T_c = 58.13 K via Eq. (3).

$$\chi = \chi_0 - \frac{1}{3} g_{eff} \frac{\pi k_B \xi_{ab}^2(0) T}{\phi_0^2 s} \frac{T_c}{T - T_c} \quad (3)$$

where χ_0 contains the normal-state contributions in the absence of fluctuations and is assumed to be independent of *T*. g_{eff} is the effective number of complex *s*-wave order parameters in the Cu-O plane, which is taken as 2 for the bilayer Cu-O planes in La2126+δ within the 2D fluctuation regime. Although it is difficult to fit the data precisely because of the slightly nonlinear behavior observed in Fig. 5a, we can nevertheless estimate the $\xi_{ab}(0)$ from Eq. (3). The fit of the data for both of the fields (300 Oe and 500 Oe) yields $\xi_{ab}(0) = 10.95 - 12.60$ Å. Table I shows the comparison of our La2126+δ crystal to the Bi2223 2D system, as well as the 3D YBCO system. La2126+δ exhibits Ginzburg-Landau coherence lengths comparable to those of Bi2223($\xi_{ab}(0) \sim 9.6$ Å) and YBCO ($\xi_{ab}(0) \sim 16$ Å) in the *ab* plane (see Table I).

In order to put the 2D superconductivity in La2126+δ in perspective, one needs to understand the structural as well as transport properties of the system in hand. Structurally, $La_2CaCu_2O_{6+\delta}$ is recognized as the simplest bilayer system.[35] $La_2CaCu_2O_{6+\delta}$ has been shown to possess Cu-O bilayers, but without the Cu-O chains present in YBCO.[35] Its unit cell comprises of two CuO_5 pyramidal planes, separated by a cation monolayer.[35] The interstitial oxygen has been shown to go on the O(3) site upon high pressure annealing (see Fig. 1), and effectively bridging the two CuO_5 pyramids in a bilayer to two CuO_6 octahedra.[28,29,33] The interstitial oxygen plays an important role on the superconductivity although the detailed role is still unclear. In addition, there are La-O and Ca-O layers between the CuO_6 octahedra, which is similar with the structure arrangement in Bi2223. Thus, from the aspect of structural properties, La2126+$\delta$is structurally closer to the 2D Bi2223 system.

High temperature superconductors possess *H* – *T* phase diagrams which are characterized by large areas where the fluctuations in the order parameter are important. As a matter of fact, the relative importance of the thermal fluctuations is given by the Ginsburg parameter, *Gi*, which is heavily determined by the coherence length, ξ, and the dimensionality of the system, *D*.[36] The correlations grow weaker at reduced dimensions,[37] thus the effect of the fluctuations is more pronounced in 2D compared to 3D, particularly when it comes to the contributions of the fluctuations to magnetization measurements.[36] Two indications which would suggest that the system is either 2D or 3D would be (*i*) the relationship between the superconducting coherence length and the spacing between the conduction planes,[38] and (*ii*) the strength of the Josephson coupling. The latter item is related to the superfluid density and its assessment is beyond the scope of the present paper.[39]

A decisive factor determining the dimensionality of a superconductor, is the field anisotropy, γ (for comparison of ξs and γs in La2126, Bi2223 and YBCO, please see Table I). As we can see, γ^{Bi2223} is much larger than γ^{YBCO} ($\gamma^{YBCO} \sim 4 - 7$)[43, 44] or γ^{La2126} ($\gamma^{La2126} \sim 7$)[40], leading to the extremely small *c*-axis coherence length, $\xi_c(0)$, observed in Bi2223($\xi_c^{Bi2223}(0) \sim$ 0.2 Å). From the anisotropy value for La2126+δ, we can similarly estimate its $\xi_c^{La2126}(0)$,

and we show that it is around 1.65 Å (clearly lying much above $\xi_c^{Bi2223}(0)$, while being below $\xi_c^{YBCO}(0)$). In fact, the dimensionality of a superconductor can be changed by slightly changing the doping level. Such a behavior was observed by Li *et al*. in $La_{2-x}Sr_xCuO_4$ (LSCO) system,[7] which clearly showed that its dimensionality moves from 2D-like behavior to 3D-like behavior as the Sr-content increases.[7] Qualitatively speaking, increasing the charge concentration makes the system less anisotropic, and decreases the effective layer spacing.[7] In an intermediate- and strong-coupled layered superconductor, *s* may not be taken as the physical distance between two relatively weakly-coupled superconducting layers.[7] It is the effective separation including the positional correlation in the neighboring layers. However, there is no quantitative description of the relation between the crossing point magnetization and the anisotropy for a layered superconductor.[7] Most notably, the 2D to 3D crossover happens as a result of a shrinking effective s^* and/or decreasing γ (with a subsequent increase in ξ_c), suggesting the importance of the ratio of *s* to ξ_c.

It is interesting to note that the ratio of conduction interlayer separation and coherence length of a 2D system is very large, as compared to a 3D one (see Table I).[38] The interspacing distance, *s* in La2126, is again an intermediate value between the respective distances in Bi2223 and YBCO, s^{Bi2223} and s^{YBCO}. Most significantly, Bi2223 and YBCO exhibit 2D and 3D superconductivity, respectively, which would be suggested by the relation of conduction layer spacings to superconducting coherence lengths (see Table I). We can explain this by introducing the cooper pair coupling behavior as plotted in Fig. 6. In this 3D plot, it is clearly shown that a strong coupling between superconducting layers is observed in the 3D superconductor, while 2D system exhibits the separately distribution of the cooper pair coupling inside the superconducting layers. Our La2126 sample shows the crossover behavior between 2D and 3D but much closer to 2D system due to the much larger $s/\xi_c(0)$ ratio. The fluctuation character of the superconductivity in La2126 appears to be very robust unlike the one observed in *i*) MgB_2, where fluctuation effects occur at only the very low fields (H ~ 100 Oe),[45]or *ii*) Pb nanoparticles, in which case the first-order fluctuation correction is found to be valid only outside the critical region, where it accurately describes the diamagnetic magnetization for magnetic fields (only not too close to the critical field),[46] – all observations consistent with GL-LLL. Our La2126 system also did not exhibit non-conventional fluctuation diamagnetism as the one observed in some underdoped systems, such as $Y_{1-x}Ca_xBa_2Cu_3O_\delta$,[47,48] and attributed to thermally-excited vortices which need be properly accounted via a Coulomb-gas theoretical approach,[49] albeit this may be a behavior that we may anticipate to see at much lower applied fields.

IV. Conclusions:

In conclusion, the analysis of the magnetization data presented here show that the magnetization properties of a superconducting $La_{1.9}Ca_{1.1}Cu_2O_{6+\delta}$ single crystal near $T_c(H)$ in high fields can be described quite nicely by GL-LLL fluctuation theory for a 2D superconductor. The low-field fluctuation diamagnetic susceptibility $\chi(T)$ above T_c can be fitted in terms of the 2D Lawrence-Doniach model. Our findings suggest that $La_{1.9}Ca_{1.1}Cu_2O_{6+\delta}$ is a quasi-2D superconductor from the aspects of both its structural and

transport properties: it is suggested that the large anisotropy in $La_{1.9}Ca_{1.1}Cu_2O_{6+\delta}$, manifest in the large ratio between the superconducting interspacing distance and the coherence length along the *c* axis, is the cause behind the 2D nature of the fluctuation superconductivity in it. We suggest future optical spectra and μSR measurements to assess the superfluid density, i.e., the strength of the Josephson couplings between the different conduction bilayers.

Acknowledgments

This work was supported by the U.S. Department of Energy, Office of Basic Energy Science, Materials Sciences and Engineering Division, under Contract No. DE-SC00112704.

References:

[1] J. G. Bednorz and K. A. Muller, Z. Phys. B **64**, 189 (1986).
[2] D. J. Van Harlinger, Rev. Mod. Phys. **67**, 515 (1995) and references therein; Patrick A. Lee, Naoto Nagaosa, Xiao-Gang Wen, Rev. Mod. Phys. **78**, 17 (2006) and references therein.
[3] Y. Yeshurun, A. P. Malozemoff, and A. Shaulov, Rev. Mod. Phys.**68**, 911 (1996) and references therein; G. Blatter, M. V. Feigel'man, V. B. Geshkenbein, A. I. Larkin, and V. M. Vinokur, Rev. Mod. Phys.**66**, 1125 (1994) and references therein.
[4] V.V. Flambaum and O.P. Sushkov, Physica C **175**, 347 (1991).
[5] Elbio Dagotto, Rev. Mod. Phys. **66**, 763 (1994) and references therein.
[6] Andrei Mourachkine, *High-Temperature Superconductivity in Cuprates: The Nonlinear Mechanism and Tunneling Measurements*, pg. 39 – 41 (Kluwer Academic Publishers, 2002).
[7] Qiang Li, Chapter 4 Effects of Vortex and Critical Fluctuations on Magnetization of High T_c Superconductors, "*Physical Properties of High Temperature Superconductivity V*", edited by D. M. Ginsberg, (World Scientific, 1996) and references therein.
[8] P. A. Lee and S. R. Shenoy, Phys. Rev. Lett. **28**, 1025 (1972); A. Lascialfari, P. Tedesco and I. Zucca, Int. J. Mod. Phys. B **17**, 805 (2003); C Torrón, A Diaz, A Pomar, JA Veira, F Vidal, Physical Review B **49** (18), 13143 (1994); I. K. Dimitrov, W. D. Si, W. Ku, S. J. Han, and J. Jaroszynski, Low Temp. Phys. **39**, 680 (2013).
[9] U. Welp, S. Fleshler, W. K. Kwok, R. A. Klemm, V. M. Vinokur, J. Downey, B. Veal, and G. W. Crabtree, Phys. Rev. Lett. **67**, 3180 (1991);M. J. Naughton, R. C. Yu, P. K. Davies, J. E. Fischer, R. V. Chamberlin, Z. Z. Wang, T. W. Jing, N. P. Ong, and P. M. Chaikin, Phys. Rev. B **38**, 9280(R) (1998);
[10] T. T. M. Palstra, B. Batlogg, L. F. Schneemeyer, R. B. van Dover, and J. V. Waszczak, Phys. Rev. Lett. **64**, 3090 (1990).
[11] S. E. Inderhees, M. B. Salamon, J. P. Rice, and D. M. Ginsberg, Phys. Rev. Lett. **66**, 232 (1991); A Junod, M. Roulin, B. Revaz, A. Mirmelstein, J.-Y. Genoud, E. Walker, and A. Erb., Physica C **282-287**, 1399 (1997); B. Zhou, J. Buan, Stephen W. Pierson, C. C. Huang, Oriol T. Valls, J. Z. Liu, and R. N. Shelton, Phys. Rev. B **47**, 11631(R) (1993); A. Junod, K.-Q. Wang, T. Tsukamoto, B. Revaz, G. Triscone, E. Walker, and J. Muller, Physica C **235-340**, 1761 (1994);A Pomar, MV Ramallo, J Mosqueira, C Torrón, Felix Vidal, Phys. Rev. B 54, 7470 (1996)

[12] P. H. Kes, C. J. van der Beck, M. P. Maley, M. E. McHenry, D. A. Huse, M. J. V. Menken and A. A. Menovsky, Phys. Rev. Lett. **67**, 2383 (1991).
[13] K. Kadowaki, Physica C **183**-**189**, 2240 (1991).
[14] Q. Li, K. Shibutani, M. Suenaga, I. Shigaki, and R. Ogawa, Phys. Rev. B **48**, 9877 (1993).
[15] Q. Li, M. Suenaga, T. Hikata, and K. Sato, Phys. Rev. B **46**, 5857 (1992).
[16] Q. Li, M. Suenaga, L. Bulaevskii, T. Hikata, and K. Sato, Phys. Rev. B **48**, 13865 (1993).
[17] J. H. Cho, D. C. Johnston, M. Ledvij, and V. G. Kogan, Physica C **212**, 419 (1993).
[18] J. R. Thompson, J. G. Ossandon, D. K. Christen, B. C. Chakoumakos, Yang Ren Sun, and M. Paranthaman and J. Brynestad, Phys. Rev. B **48**, 14 031 (1993).

[19] L. N. Bulaevskii, M. Ledvij, and V. G. Kogan, Phys. Rev. Lett. **68**, 3773 (1992).
[20] Z. Tešanović, Lei Xing, Lev Bulaevskii, Qiang Li, and M. Suenaga, Phys. Rev. Lett. **69**, 3563 (1992).
[21] V. G. Kogan, M. Ledvij, A. Yu. Simonov, J. H. Cho, and D. C. Johnston, Phys. Rev. Lett. **70**, 1870 (1993).
[22] J. Mosqueira, R. I. Rey, A. Wahl, and F. Vidal, Phys. Rev. B **84**, 134504 (2011).
[23] Qiang Li, M. Suenaga, G. D. Gu, and N. Koshizuka, Phys. Rev. B **50**, 6489 (1994).
[24] G. D. Gu, M. Hücker, Y.-J. Kim, J. M. Tranquada, H. Dablowska, G. M. Luke, T. Timusk, B. D. Gaulin, Q. Li, and A. R. Moodenbaugh, J. Phys. Chem. Solids **67**, 431 (2006).
[25] Y. Hirata, K. M. Kojima, M. Ishikado, S. Uchida, A. Iyo, H. Eisaki, and S. Tajima, Phys. Rev. B **85**, 054501 (2012).
[26] A. Palau, T. Puig, X. Obradors, and Ch. Jooss, Phys. Rev. B **75**, 054517 (2007).
[27] B. I. Belevtsev, E. Yu. Beliayev, D. G. Naugle, K. D. D. Rathnayaka, M. P. Anatska, and I. Felner, J. Phys.: Condens. Matter **19**, 036222 (2007).
[28] K. Kinoshita and T. Yamada, Phys. Rev. B **46**, 9116 (1992).
[29] H. Shaked, J. D. Jorgensen, B. A. Hunter, R. L. Hitterman, K. Kinoshita, F. Izumi, and T. Kamiyama, Phys. Rev. B **48**, 12 941 (1993).
[30] S. Ullah and A. T. Dorsey, Phys. Rev. Lett. 65, 2066 (1990); S. Ullah and A. T. Dorsey, Phys. Rev. B **44**, 262 (1991).
[31] H. Maeda, Y. Tanaka, M. Fukutumi, and T. Asano, Jpn. J. Appl. Phys.**27** (2): L209–L210 (1998).
[32] R. A. Klemm, Phys. Rev. B **41**, 2073 (1990).
[33] M. Hücker, Young-June Kim, G. D. Gu, J. M. Tranquada, B. D. Gaulin, and J. W. Lynn, Phys. Rev. B **71**, 094510 (2005).
[34] C. Ulrich, S. Kondo, M. Reehuis, H. He, C. Bernhard, C. Niedarmayer, F. Bourée, P. Bourges, M. Ohl, H. M. Rønnow, H. Takagi, and B. Keimer, Phys. Rev. B **65**, 220507 (2002).
[35] R. J. Cava, Science **247**, 656 (1990).
[36] B. Rosenstein, B. Ya. Shapiro, R. Prozorov, A. Shaulov, and Y. Yeshurun, Phys. Rev. B **63**, 134501 (2001).
[37] R. Peierls, *Surprises in Theoretical Physics*, (Princeton University Press, 1979).
[38] We take the value of the interlayer spacing s for the calculation of s^*/ξ as an indication of 2D behavior in lieu of the effective interlayer separation, s^*.
[39] Y. Hirata, K. M. Kojima, M. Ishikado, S. Uchida, A. Iyo, H. Eisaki, and S. Tajima, Phys. Rev. B **85**, 054501 (2012).

[40] M. Okuya, T. Kimura, R. Kobayashi, J. Shimoyama, K. Kitazawa, K. Yamafuji, K. Kishio, K. Kinoshita, and T. Yamada, J. Supercond. **7**, 313 (1993).
[41] D. E. Farrell, S. Bonham, J. Foster, Y. C. Chang, P. Z. Jiang, K. G. Vandervoot, D. J. Lam, and V. G. Kogan, Phys. Rev. Lett. **63**, 782 (1989).
[42] W. C. Lee, J. H. Cho, and D. C. Johnston, Phys. Rev. B **43**, 457 (1991).
[43] U. Welp, W. K. Kwok, G. W. Crabtree, K. G. Vandervoort, and J. Z. Liu, Phys. Rev. Lett. **62**, 782 (1908).
[44] D. E. Darrell, J. P. Rice, and D. M. Ginsberg, J. Z. Liu, Phys. Rev. Lett. **64**, 1573 (1990).
[45] A. Lascialfari, T. Mishonov, A. Rigamonti, P. Tedesco, and A. Varlamov, Phys. Rev. B **65**, 180501(R) (2002).
[46] E. Bernardi, A. Lascialfari, A. Rigamonti, L. Romanò, V. Iannotti, G. Ausanio, and C. Luponio, Phys. Rev. B **74**, 134509 (2006).
[47] A. Lascialfari, A. Rigamonti, L. Romano', A. A. Varlamov, and I. Zucca, Phys. Rev. B **68**, 100505(R) (2003).
[48] A. Lascialfari,1 A. Rigamonti,1 L. Romano',2 P. Tedesco,1 A. Varlamov,3 and D. Embriaco4, Phys. Rev. B **65**, 144523 (2002); E. Bernardi, A. Lascialfari, A. Rigamonti, L. Romanò, M. Scavini, and C. Oliva, Phys. Rev. B **81**, 064502 (2010).
[49] Alain Sewer and Hans Beck, Phys. Rev. B **64**, 014510 (2001).

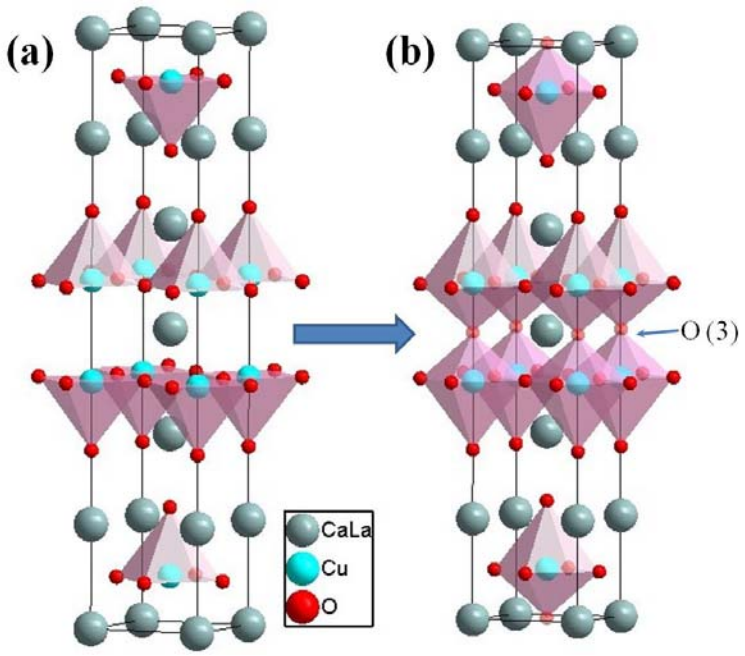

Fig.1 (color online) Crystal structure of (a) $La_2CaCu_2O_6$ and (b) $La_2CaCu_2O_{6+\delta}$.

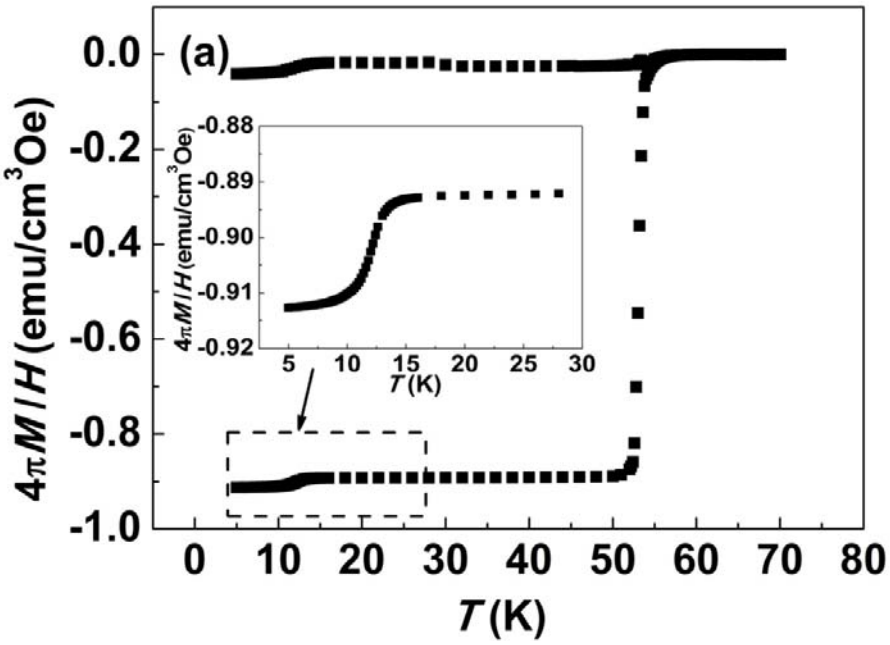

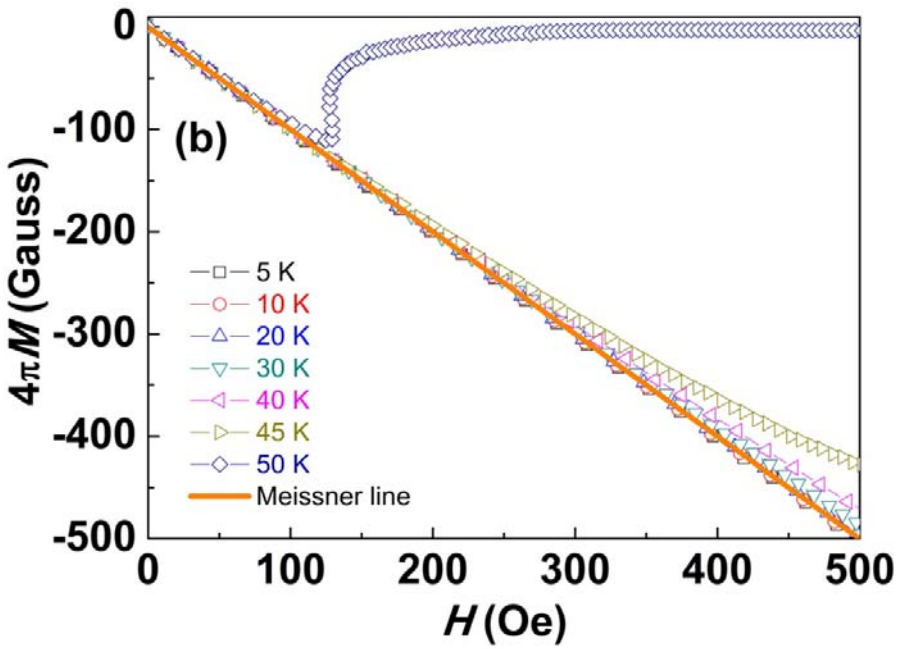

Fig. 2 (color online) (a)Temperature dependence of the magnetic susceptibility of $La_{1.9}Ca_{1.1}Cu_2O_{6+\delta}$.(b) Low-field parts of $M(H)$ at various temperature for $H\|c$ with demagnetization correct, respectively. The solid line is the "Meissner line". Here, the field H is equal to $H_a - NM$, which has already taken into account the demagnetization factor N at applied field $H_a = 2$ Oe.

Table I. Superconducting transition temperature T_c, anisotropy γ, Ginzberg-Landau coherence length in the *ab* plane [ξ_{ab} (0)] and along the *c* axis [ξ_c (0)], superconducting interspacing distance *s* and superconducting volume fractions in a particular *quasi*-2D superconductor M^*/M^{*th} for $La_{1.9}Ca_{1.1}Cu_2O_6$, $Bi_2Sr_2CaCu_2O_8$, $Bi_2Sr_2Ca_2Cu_3O_{10}$ and $YBa_2Cu_3O_{7-\delta}$. All the data from comparison samples is from literature. The Ginzberg-Landau coherence length along *c* axis ξ_c (0) of our crystal is calculated through the anisotropy data reported in the ref.40. The superconducting volume fraction of $YBa_2Cu_3O_{7-\delta}$ was estimated and calculated using the data from ref.9.

Compounds	T_c (K)	γ	ξ_{ab} (0) (Å)	ξ_c (0) (Å)	*s* (Å)	M^*/M^{*th}
$La_{1.9}Ca_{1.1}Cu_2O_{6+\delta}$	53.5	7.1[40]	11.8±0.9	1.65 (cal)	9.8	29.8 %
$Bi_2Sr_2CaCu_2O_8$[14, 41, 42]	84.2	>50	20.4	0.37	15.395	82 %
$Bi_2Sr_2Ca_2Cu_3O_{10}$[15]	107.5	>50	9.6	0.2	18.6	60 %
$YBa_2Cu_3O_{7-\delta}$[9, 43]	92.1	~5.3	16	3	5.8	<10% (cal)

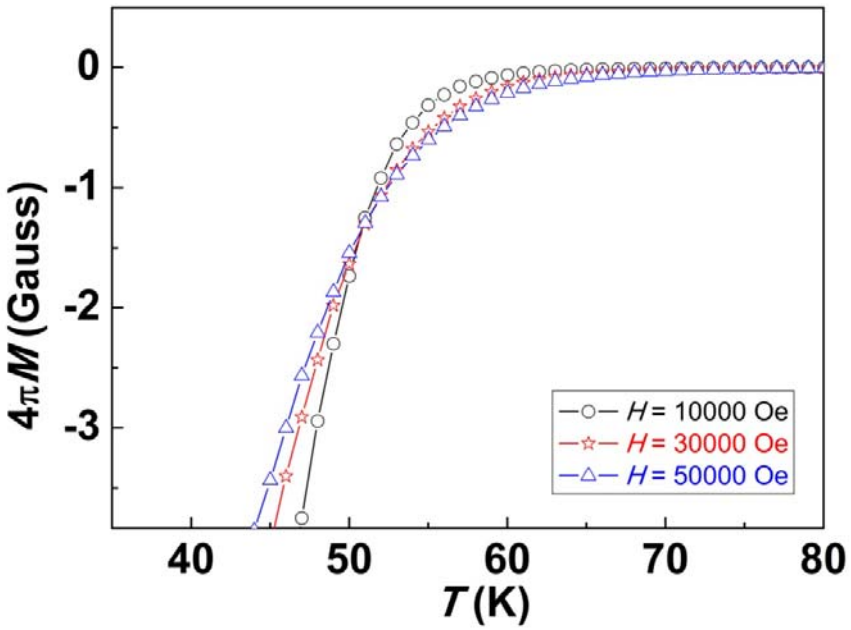

Fig. 3 (color online) Temperature dependence of the magnetization of $La_{1.9}Ca_{1.1}Cu_2O_{6+\delta}$ in various magnetic fields parallel to the *c* axis.

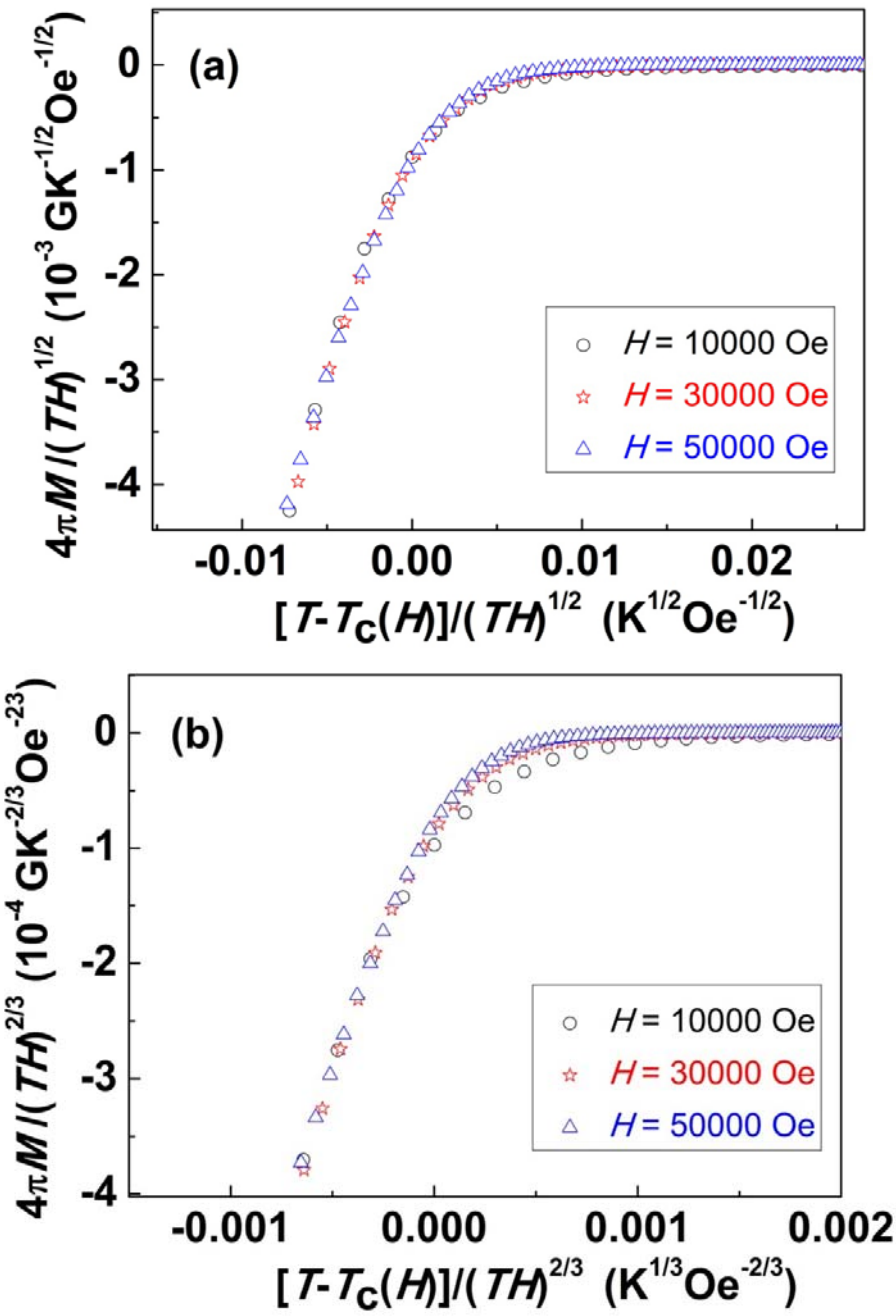

Fig. 4 (color online) (a) 2D scaling of the magnetization data for $La_{1.9}Ca_{1.1}Cu_2O_{6+\delta}$ measured at 10000, 30000, and 50000 Oe with magnetic fields parallel to the *c* axis. (b) 3D scaling of the same magnetization data as shown in (a).

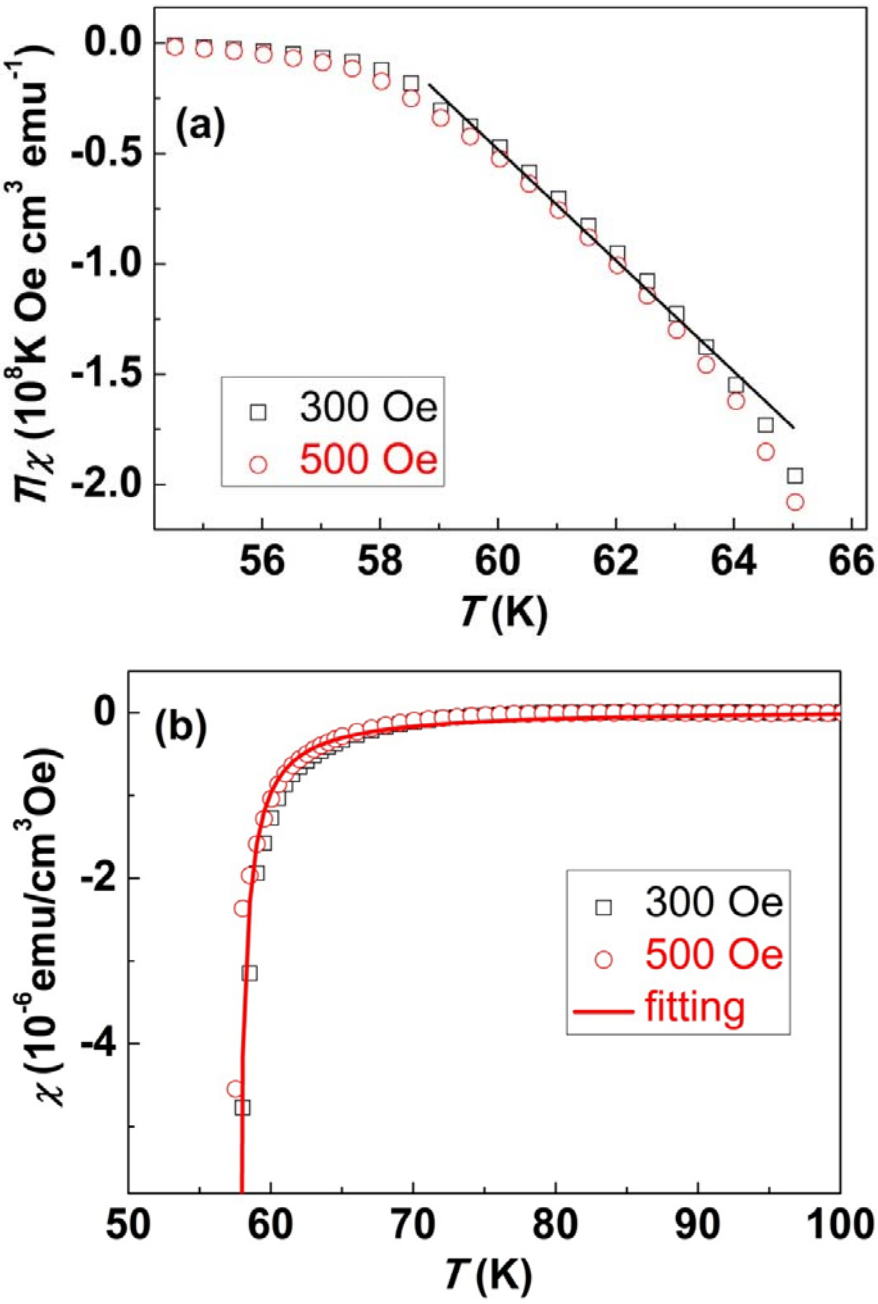

Fig. 5.(color online) Temperature dependence of T/χ (a) and χ (b), measured at 300 Oe and 500 Oe. The solid line in (a) represents the linear fit of the data and the solid curve in (b) is a theoretical fit to the data of 300 Oe using Eq. (3).

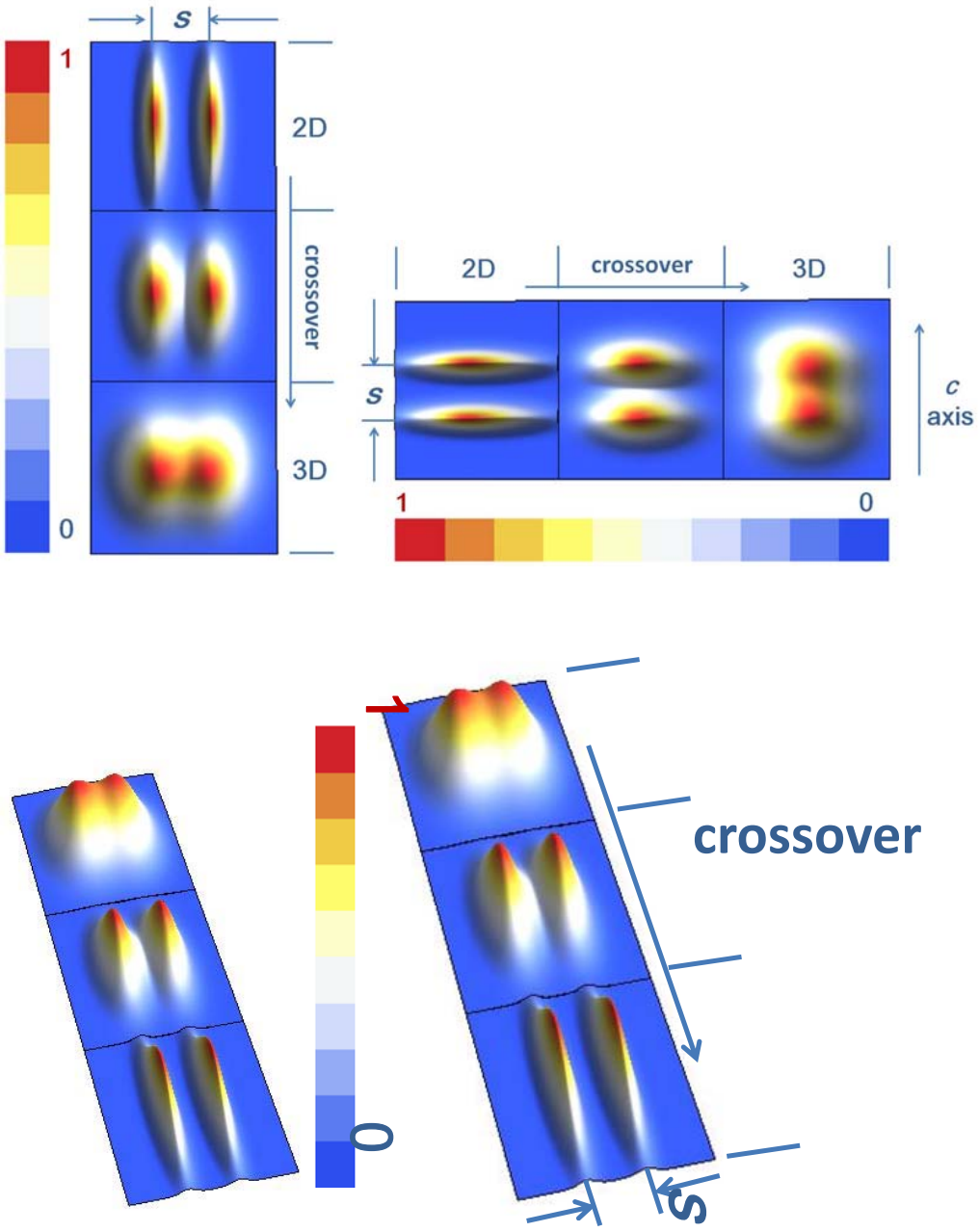

Fig. 6. 3D plot of Cooper pair coupling behavior based on the data listed in Table I. We choose $Bi_2Sr_2Ca_2Cu_3O_{10}$, $La_{1.9}Ca_{1.1}Cu_2O_{6+\delta}$ in this paper and $YBa_2Cu_3O_{7-\delta}$ for 2D, 2D to 3D crossover and 3D behavior, respectively. Here, we fix the interspacing distance between layers s for all the samples and ξ_c (0) changes according to the ratio of ξ_c (0)/s listed in Table I. The anisotropy value γ is applied to decide ξ_{ab} (0). The different colors represent the electron concentration levels, where the red part means the highest concentration (set to 1 in the color bar) and the dark blue (set to be 0 in the color bar) shows the lowest concentration. The pictorial representation where the overlap is the greatest corresponds to the 3D system where the coherence length is longer than the interlayer spacing, while the one where the two lobes

are completely separated corresponds to the *bona fide* 2D case with the crossover scenario being in the middle.